

Optimum pinning of the vortex lattice in extremely type-II layered superconductors

C. E. Creffield¹ and J. P. Rodriguez²

¹*Instituto de Ciencia de Materiales (CSIC), Cantoblanco, E-28049 Madrid, Spain**

²*Dept. of Physics and Astronomy, California State University, Los Angeles, California 90032, USA*

(Dated: November 4, 2018)

The two-dimensional (2D) vortex lattice in the extreme type-II limit is studied by Monte Carlo simulation of the corresponding 2D Coulomb gas, with identical pins placed at sites coinciding with the zero-temperature triangular vortex lattice. At weak pinning we find evidence for 2D melting into an intermediate hexatic phase. The strong pinning regime shows a Kosterlitz-Thouless transition, driven by interstitial vortex/anti-vortex excitations. A stack of such identical layers with a weak Josephson coupling models a layered superconductor with a triangular arrangement of columnar pins at the matching field. A partial duality analysis finds that layer decoupling of the flux-line lattice does not occur at weak pinning for temperatures below 2D melting.

I. INTRODUCTION

It is well known that the motion of vortex lines in the mixed phase of a type-II superconductor generates dissipation, and hence that an unpinning vortex-lattice state is in fact resistive¹. This has been confirmed recently in the mixed phase of clean high-temperature superconductors, where the superconductivity of samples with a strip geometry is found to be very much superior to that in samples with a Corbino disk geometry². Surface barriers in the strip geometry prohibit rigid motion of the vortex lattice, while the Corbino disk geometry allows for rigid rotations of the vortex lattice. The above phenomena can be understood theoretically in the extreme type-II limit, where magnetic screening is absent¹. Rigid translations of the vortex lattice result in an infrared divergence that destroys phase coherence at any temperature³. This infrared divergence can be removed by excluding rigid motion of the vortex lattice through surface barriers, whereupon phase coherence is restored⁴.

Defects in the bulk of a superconductor can also effectively prohibit the rigid motion of the vortex lattice¹. In this work we study the nature of phase coherence in an extremely type-II layered superconductor, with magnetic field oriented perpendicular to the layers, and containing an array of correlated pins. We choose to use an optimum arrangement of identical columnar pins⁵, the locations of which match the triangular vortex lattice at zero temperature. Such a configuration can be realized experimentally by artificial “anti-dot” arrays⁶. The Josephson coupling between layers is turned off initially, thus allowing us to model the system of vortices in each layer by a two-dimensional (2D) Coulomb gas with a uniform charge background and a commensurate pinning potential. (cf. ref. 7) We employ Monte Carlo (MC) simulations to uncover the thermodynamic phase diagram of this system under periodic boundary conditions. The depth of the pinning potential, U , becomes a useful control parameter. As U increases from zero, the “floating” vortex lattice phase^{8,9} that exists at $U = 0$ becomes pinned at a critical U_p . A finite-size analysis shows that U_p tends to zero in the thermodynamic limit, and that

floating is prohibited initially by a sparse distribution of pinned vortices. Phase coherence is then restored at a yet stronger pinning, U_m . The vortex lattice inside the range $U_p < U < U_m$ therefore shows no phase coherence despite the fact that it does not float! The identification of this regime with the *hexatic* phase¹⁰ is indicated by recent theoretical work⁴. Indeed, a modest size analysis demonstrates that this phase shows (strict) long-range orientational order, which is a hallmark of the hexatic phase¹⁰. The strong-pinning regime at the other extreme exhibits a standard Kosterlitz-Thouless (KT) transition driven by the unbinding of vortex/anti-vortex pairs that are *not* linked to the vortex lattice¹¹, which is now fixed to the pins and appears to be irrelevant¹². Lastly, the effects of a weak Josephson coupling between layers is determined through the application of a partial duality analysis of the corresponding layered XY model¹². On this basis, we conclude that the superconducting-normal transition shown by such an optimally pinned vortex lattice lies within the universality class of the three-dimensional (3D) XY model.

II. 2D VORTEX LATTICE WITH COMMENSURATE PINS

Consider an infinite stack of isolated superconducting layers in a perpendicular external magnetic field. Each layer is assumed to be identical in order to reflect the correlated pinning. A weak Josephson coupling will be switched on later. Magnetic screening effects can be neglected in the extreme type-II limit assumed throughout, in which case the XY model over the square lattice with uniform frustration provides a qualitatively correct description of the mixed phase of each layer. The corresponding Boltzmann distribution is set by the energy functional

$$E_{XY}^{(2)} = - \sum_{\mu=x,y} \sum_{\vec{r}} J_{\mu}(\vec{r}) \cos[\Delta_{\mu}\phi(\vec{r}) - A_{\mu}(\vec{r})] \quad (1)$$

for the superfluid kinetic energy in terms of the superconducting phase $\phi(\vec{r})$. Here $\Delta_{\mu}\phi(\vec{r}) = \phi(\vec{r} + a\hat{\mu}) - \phi(\vec{r})$

and $\vec{A} = (0, 2\pi f x/a)$ make up the local supercurrent, where f denotes the concentration of vortices over the square lattice, with lattice constant a . The local phase rigidity $J_\mu(\vec{r})$ is assumed to be constant over most of the nearest-neighbor links $(\vec{r}, \vec{r} + a\hat{\mu})$, with the exception of those links in the vicinity of a pinning site. We shall next

take the Villain approximation which is generally valid at low temperature^{13,14}. After making a series of standard manipulations, we obtain a Coulomb gas ensemble with pins that describes the vortex degrees of freedom on the dual square lattice. The ensemble is weighted by the Boltzmann distribution set by the energy functional

$$E_{\text{vx}} = (2\pi)^2 \sum_{(\vec{R}_1, \vec{R}_2)} [Q(\vec{R}_1) - f] JG^{(2)}(\vec{R}_1, \vec{R}_2) [Q(\vec{R}_2) - f] + \sum_{\vec{R}} V_p(\vec{R}) |Q(\vec{R})|^2, \quad (2)$$

in terms of the integer vorticity field $Q(\vec{R})$ over the sites \vec{R} of the dual lattice. The logarithmic interaction between the vortices can be expressed as a Greens function $JG^{(2)} = \sum_n |n\rangle \varepsilon_n \langle n|$, where the states $|n\rangle$ diagonalize the operator $-\sum [J_x^{-1} \Delta_y^2 + J_y^{-1} \Delta_x^2]$ with corresponding eigenvalues ε_n^{-1} . Here, the lattice difference operator $\Delta_{y(x)}$ acts between those adjacent points on the dual lattice that are split by the link on the base lattice that the coupling constant $J_{x(y)}$ refers to. The effective coupling energy J is set by the requirement that $\langle \vec{q}_1 | G^{(2)} | \vec{q}_2 \rangle = q_1^{-2} a^{-2} \delta_{1,2}$ for plane waves $|\vec{q}_i\rangle$ in the long wavelength limit, $q_i \rightarrow 0$. The pinning potential, on the other hand, originates from the contribution to the former Greens function by bound states localized at the pinning sites: $V_p(\vec{R}) = (2\pi)^2 \sum_{\varepsilon_n < 0} \varepsilon_n |\langle \vec{R} | n \rangle|^2$. Finally it is instructive to point out that the phase rigidity can also be directly computed within the Villain approximation, where it is given by¹⁵ one over the dielectric constant of the Coulomb gas ensemble (2). In particular, for an $L \times L$ square mesh with periodic boundary conditions, we have

$$\rho_s/J = 1 - \lim_{k \rightarrow 0} (2\pi)^2 \beta \left(\langle Q_{\vec{k}} Q_{-\vec{k}} \rangle - \langle Q_{\vec{k}} \rangle \langle Q_{-\vec{k}} \rangle \right) / k^2 a^2 L^2, \quad (3)$$

where $\beta = J/k_B T$ is the inverse temperature of the system, and $Q_{\vec{k}} = \sum_{\vec{R}} Q(\vec{R}) e^{i\vec{k} \cdot \vec{R}}$ is the Fourier transform of the charge density.

To proceed further, we shall first replace the Greens function mediating the interaction between vortices in Eq. (3) with the standard one $G^{(2)} = -\nabla^{-2}$ over the square lattice subject to periodic boundary conditions^{13,14}. This approximation neglects only the short-range features of the interaction energy near the pinning centers. Secondly, we shall consider the optimum pinning configuration: $V_p(\vec{R}) = -U$ for points \vec{R} that coincide with the triangular vortex lattice at zero temperature, and $V_p(\vec{R}) = 0$ otherwise. The long-range logarithmic interaction among vortices enforces charge neutrality with the uniform background charge density f , such that:

$$\sum_{\vec{R}} Q(\vec{R}) = f L^2. \quad (4)$$

This means that the system of vortices is incompressible at all temperatures. Vacancies and interstitials are therefore impossible at long wavelengths. In the absence of extrinsic pins^{8,9}, $U = 0$, and at low vorticity, $f < 1/30$, the triangular vortex-lattice depins from the underlying square lattice at a temperature $k_B T_p^{(0)} = 1.5 f J$. At higher temperatures it “floats”, before melting at $k_B T_m^{(0)} = J/20$. At low vorticity and low temperature, the difference in the internal energy between the floating and the pinned vortex lattice phases is therefore $\Delta E = N_{\text{vx-p}} U$, where $N_{\text{vx-p}}$ denotes the average number of pinned vortices. The corresponding difference in the entropy is $\Delta S = k_B \ln(2/f)$, which is not extensive. The balance in free energy, $\Delta E = T \Delta S$, yields a (first-order) transition between the two phases at a critical pinning strength

$$U_p = N_{\text{vx-p}}^{-1} k_B T \ln(2/f) \quad (5)$$

that vanishes in the thermodynamic limit, $L \rightarrow \infty$. Below we shall confirm this prediction at weak pinning, as well as exploring the effect of strong pinning through MC simulation of the 2D Coulomb gas ensemble (2).

The following thermodynamic quantities are measured in the MC simulations of the Coulomb gas ensemble (2) describing a 2D vortex lattice with optimum pins. Phase coherence is probed by the superfluid stiffness (3). Pinning of the vortex lattice is determined by checking for the appearance of Bragg peaks in the vortex density, $S_0(\vec{k}) = |\langle Q_{\vec{k}} \rangle|^2$. This is quantified by taking the ratio between the heights of the first-order and zero-order Bragg peaks, which we term the “Bragg ratio”. *Intrinsic* positional correlations among the vortices, on the other hand, are measured through the fluctuation contribution to the structure function, $S_1(\vec{k}) = \langle Q_{\vec{k}} Q_{-\vec{k}} \rangle - \langle Q_{\vec{k}} \rangle \langle Q_{-\vec{k}} \rangle$. Lastly we also measure the six-fold orientational order parameter characteristic of the triangular vortex lattice:⁸⁻¹⁰ $\phi_6 = N_{\text{vx}}^{-2} \sum_{j,k} \langle \exp[6i(\theta_j - \theta_k)] \rangle$. Here θ_j is the angle between a fixed direction in space and the direction of the bond between the j -th vortex and its nearest neighbor. In general, this orientational order parameter decays algebraically with system size as $L^{-\eta_6}$ in the thermodynamic limit, $L \rightarrow \infty$. The correlation

exponent η_6 is null in the case of a 2D vortex lattice with strict long-range order, while $\eta_6 = 2$ if only short-range orientational order exists⁹.

The MC scheme used closely follows that developed by Lee and Teitel¹⁶. A single MC move consists of selecting a lattice point and one of its nearest neighbors at random, and adding a unit charge to one of the points and subtracting unit charge from the other, thereby keeping the total charge of the system constant. This alteration is then either accepted or rejected according to the standard Metropolis algorithm. At temperatures lower than $J/4k_B$, simulations revealed that the accepted configurations *only* possessed charges of $Q = +1$, the total number of charges, N_{vx} , being set by overall charge neutrality (4). All other configurations, such as those with multiple or negative charges, were heavily penalized on energetic grounds. This permits a much less computationally costly MC move to be employed in this regime, which consists of selecting one of these N_{vx} charges at random and moving it to an unoccupied neighboring lattice site. Extensive simulations at low temperatures were run using both MC updating methods to confirm that they indeed gave the same results, and thereafter the second algorithm was used to obtain the bulk of the low-temperature results in this paper. The MC estimates are based on between 8000 and 12000 measurements, following an equilibration from a random initial configuration consisting of 8000 MC sweeps. In all cases this process was repeated a number of times, using a different initial state, to ensure that the simulations were not becoming ergodically trapped.

Fig. 1 displays temperature profiles of the various physical probes that were listed above, for three different regimes of the strength of the pinning potential. The phase-incoherent floating phase lies in between the pinned vortex lattice and the vortex liquid as a function of temperature in the no-pinning regime shown in Fig. 1a^{8,9}. A strange phase-incoherent state that does *not* float, on the other hand, lies in between the conventional solid and liquid phases in the weak-pinning regime (Fig. 1b). Table I demonstrates that this observation is not a spurious size effect. Notice, in particular, how the orientational order parameter ϕ_6 and the magnitude of the first-order Bragg peak saturate with increasing size, and how the phase rigidity remains null throughout. The former implies that the “strange” vortex phase exhibits *strict* long-range orientational order, with a correlation exponent $\eta_6 = 0$.⁹ Fig. 2 displays the resulting phase diagram in the U - T plane. The boundary, $U_p(T)$, that separates the floating phase (I) and the “strange” phase (II) extrapolates to zero roughly as L^{-1} at fixed temperature. This was determined from MC simulations at a temperature $k_B T/2\pi J = 0.0060$ for two different sizes, $L = 56$ and 112, with the addition of the thermodynamic limit, $L \rightarrow \infty$, under the assumption that $U_p = 0$ there. (Note that our MC simulations show metastability in the vicinity of this first-order pinning transition,

L	ρ_s/J	Bragg ratio	ϕ_6
56	0.001 ± 0.002	0.329 ± 0.061	0.603 ± 0.008
112	0.000 ± 0.001	0.765 ± 0.003	0.677 ± 0.002
168	0.001 ± 0.001	0.784 ± 0.003	0.690 ± 0.003

TABLE I: Finite size study of the Coulomb gas at a temperature $k_B T/2\pi J = 0.0065$ and pinning potential $U/2\pi J = 0.002$ inside the putative hexatic phase. This strength of pinning is slightly larger than U_p for $L = 56$, which explains the relatively small Bragg ratio at this size (recall that U_p decreases with size).

which reflects the two-fold orientational degeneracy of the floating states.) Consistent with the simple balance of free energy (5), we then conclude that the floating phase exists only in the absence of extrinsic pins ($U = 0$) in the thermodynamic limit. The last size analysis also implies by Eq. (5), that the number of pinned vortices in the “strange” phase scales as $N_{vx-p} \propto L$, which is *subthermodynamic*. Finally, at yet stronger pinning, the line $U = U_m(T)$ along which macroscopic phase coherence sets in shows only minor size dependence for the three $L \times L$ lattices that we simulated.

A recent theoretical analysis of the 2D Coulomb gas (2) in the absence of bulk pinning finds that an intermediate *hexatic* phase can indeed exist if rigid translations of the vortex-lattice are prohibited⁴. This phase contains unbound dislocations that generate appreciable fluctuations in the center of mass of the 2D vortex lattice. These fluctuations are responsible for both the destruction of macroscopic shear rigidity and of macroscopic phase coherence at a 2D melting transition. The hexatic phase contrasts with the conventional pinned vortex-lattice phase that shows phase coherence. It also differs from the vortex liquid phase by the presence of orientational order¹⁰. We propose to identify the strange intermediate phase (II) that neither floats nor shows macroscopic phase coherence, but that exhibits strict long-range orientational order (see Figs. 1 and 2, and Table I), with such a hexatic phase. Fig. 3 displays the fluctuation part of the structure function, $S_1(\vec{k})$, in the putative hexatic phase found in the weak-pinning regime. It shows six-fold symmetric Bragg peaks of low order, which strikingly resemble those obtained experimentally in real-life hexatic phases¹⁷. Further, Fig. 4 shows a typical configuration of the vortex lattice in the putative hexatic phase near the pinning threshold. We may note the presence of an unbound dislocation and the small fraction of vortices that are pinned. The strict long-range orientational order (Fig. 1b), the six-fold pattern shown by this intrinsic structure function (Fig. 3), and the presence of unbound dislocations (Fig. 4) are all consistent with the identification of the “strange” vortex lattice with a hexatic phase over a commensurate substrate¹⁰.

The vortex lattice tends to be fixed to each and every commensurate pin at strong $U/2\pi J > 0.01$ (see Fig. 2).

Interstitial vortex/anti-vortex excitations are the only remaining degrees of freedom in such case. The temperature dependence of the phase rigidity (3) obtained from our MC simulations strongly resembles that of the zero-field case ($f = 0$) with no extrinsic pins ($U = 0$)⁹. In particular, Fig. 1c shows how ρ_s decreases smoothly from J to 0 at the expected KT transition temperature¹¹, $k_B T_c^{(0)} \cong \frac{\pi}{2} J$. The vortex lattice subsequently frees itself from the extrinsic pins at a higher temperature, T_p , as shown by Figs. 1 and 2.

III. 3D VORTEX LATTICE WITH OPTIMUM COLUMNAR PINS

We finally apply the above results to the question of phase coherence in the vortex-lattice phase of layered superconductors. In the extreme type-II limit, this system can be modeled by an infinite stack of XY -model layers with uniform frustration, Eq. (1), but with an additional Josephson coupling, $J_z = J/\gamma'^2$, between all nearest-neighbors across adjacent layers. Also, in this limit the magnetic coupling to vortices in adjacent layers can be accounted for by weak optimum columnar pinning, $V_p(\vec{R})$, within the “substrate potential” approximation⁷. Such a layered XY model can be analyzed through a partial duality transformation that is ideally suited to the weak-coupling limit. This leads to the following partition function that encodes the thermodynamics of the coupled system: $Z_{CG} = \sum_{\{n_z\}} (\beta/2\gamma'^2)^{N[n_z]} \prod_l C[p_l]$, where $n_z(\vec{r}, l)$ is an integer link field on 2D points \vec{r} between adjacent layers l and $l + 1$ ¹². Here $C[p_l] = \langle \exp[i \sum p_l(\vec{r}) \phi(\vec{r}, l)] \rangle_{J_z=0}$ is the phase auto-correlation function of an isolated layer l probed at the dual charge that collects onto that layer: $p_l(\vec{r}) = n_z(\vec{r}, l-1) - n_z(\vec{r}, l)$. Also, $N[n_z]$ counts the total number of dual charges, $n_z = \pm 1$. The latter system is dilute in the weak-coupling limit reached at large model anisotropy parameters, $\gamma' \rightarrow \infty$. It has been shown recently by one of us⁴ that the phase auto-correlator for a pure 2D vortex lattice that cannot move rigidly has the form $|C(1, 2)| = (\rho_s/J)(r_0/r_{12})^{\eta_{2D}}$, with a small 2D correlation exponent, $\eta_{2D} < (28\pi)^{-1}$. Here r_0 is of the order of the inter-vortex spacing and r_{12} denotes the separation between the two probes. Since commensurate pinning, $V_p(\vec{R})$, increases phase coherence (see Fig. 1), the previous bound on η_{2D} continues to hold. Yet the application of the above duality analysis yields a phase rigidity across layers equal to¹² $\rho_s^\perp = (\rho_s/\gamma'^2)(r_0/\gamma'a)^{\eta_{2D}}$. The extremely small bound on η_{2D} then implies that a decoupling crossover, $\rho_s^\perp \ll \rho_s/\gamma'^2$, occurs only for astronomically large anisotropy, $f\gamma'^2 > 10^{38}$. This indicates that layer decoupling does not occur in practice in the vortex-lattice phase of extremely type-II layered superconductors at temperatures below 2D melting (cf. ref. 7).

The above partial duality analysis of course also applies directly to the question of optimum columnar pinning in

the vortex-lattice phase of strongly type-II layered superconductors. In the strong pinning regime, Fig. 1c, our MC simulation results for a single layer find conclusive evidence for a standard KT phase transition driven by the unbinding of interstitial vortex/anti-vortex pairs. This implies that the autocorrelation functions $C[p]$ that appear in Z_{CG} are precisely those corresponding to the 2D XY model in the absence of frustration ($f = 0$) and extrinsic pinning ($U = 0$), up to a gauge transformation. We thereby conclude that the strongly pinned vortex lattice at the matching field goes through a superconducting/normal transition that is second-order, and that coincides with the universality class of the standard 3D XY model.

IV. DISCUSSION AND CONCLUSIONS

In summary, we have studied the nature of phase coherence in the 2D vortex lattice at the extreme type-II limit with identical commensurate pins through Monte Carlo simulation of the corresponding 2D Coulomb gas, Eq. (2). Our most striking result is the identification of a strange intermediate phase (II) that is pinned, but that shows no macroscopic phase coherence. It lies in the midst of a floating vortex lattice, a pinned vortex lattice, and a vortex liquid phase (see Fig. 2). A recent calculation has indicated that an intermediate hexatic phase with such characteristics is indeed expected in the 2D vortex lattice at the extreme type-II limit (1) if rigid translations of the vortex lattice are prohibited⁴. The present calculations show that an arbitrarily weak array of commensurate pins have this effect in the thermodynamic limit [see Eq. (5) and Fig. 2]. We have proposed, in conclusion, that the strange intermediate phase just mentioned is in fact a hexatic vortex lattice.

On the contrary, theoretical calculations of 2D lattice melting in the presence of a weak commensurate substrate potential do *not* predict the existence of separate liquid and hexatic phases¹⁰. It is quite possible, then, that the transition that we observe through Monte Carlo simulation between a hexatic vortex lattice (II) that is pinned and a vortex liquid that is not pinned is in fact a sharp cross-over transition. In such case, the phase diagram shown in Fig. 2 would be topologically equivalent to that predicted by theory (see Ref.¹⁰, Fig. 4, right-hand side). More extensive Monte Carlo simulations may be needed to settle this question.

Acknowledgments

The authors thank R. Markiewicz, F. Nori, F. Guinea, R. Mulet and E. Altshuler for valuable discussions. CEC acknowledges support from the EU TMR programme. JPR acknowledges the hospitality of the Instituto de Ciencia de Materiales de Madrid, where this work was initiated.

-
- * Current address: Dipartimento di Fisica, Università di Roma “La Sapienza”, Piazzale Aldo Moro 2, I-00185 Roma, Italy
- ¹ M. Tinkham, *Introduction to Superconductivity* (McGraw-Hill, New York, 1996) Chap. 5.
 - ² S.F.W.R. Rycroft, R.A. Doyle, D.T. Fuchs, E. Zeldov, R.J. Drost, P.H. Kes, T. Tamegai, S. Ooi and D.T. Foord, Phys. Rev. B **60**, R757 (1999).
 - ³ K. Maki and H. Takayama, Prog. Theor. Phys. **46**, 1651 (1971); M.A. Moore, Phys. Rev. B **45**, 7336 (1992).
 - ⁴ J.P. Rodriguez, Phys. Rev. Lett. **87**, 207001 (2001).
 - ⁵ G. Blatter, M.V. Feigel'man, V.B. Geshkenbein, A.I. Larkin, and V.M. Vinokur, Rev. Mod. Phys. **66**, 1125 (1994).
 - ⁶ K. Harada, O. Kamimura, H. Kasai, T. Matsuda, A. Tonomura and V.V. Moshchalkov, Science **274**, 1167 (1996).
 - ⁷ M.J.W. Dodgson, V.B. Geshkenbein and G. Blatter, Phys. Rev. Lett. **83**, 5358 (1999).
 - ⁸ Søren A. Hattel and J.M. Wheatley, Phys. Rev. B **51**, 11951 (1995).
 - ⁹ M. Franz and S. Teitel, Phys. Rev. B **51**, 6551 (1995).
 - ¹⁰ D.R. Nelson and B.I. Halperin, Phys. Rev. B **19**, 2457 (1979).
 - ¹¹ J.M. Kosterlitz and D.J. Thouless, J. Phys. C **6**, 1181 (1973).
 - ¹² J.P. Rodriguez, Phys. Rev. B **62**, 9117 (2000); Physica C **332**, 343 (2000); Europhys. Lett. **54**, 793 (2001).
 - ¹³ J.V. José, L.P. Kadanoff, S. Kirkpatrick and D.R. Nelson, Phys. Rev. B **16**, 1217 (1977).
 - ¹⁴ C. Itzykson and J. Drouffe, *Statistical Field Theory*, Vol. 1, (Cambridge Univ. Press, Cambridge, 1991) chap. 4.
 - ¹⁵ P. Minnhagen and G.G. Warren, Phys. Rev. B **24**, 2526 (1981); P. Minnhagen, Rev. Mod. Phys. **59**, 1001 (1987).
 - ¹⁶ Jong-Rim Lee and S. Teitel, Phys. Rev. B **46**, 3247 (1992).
 - ¹⁷ R. Seshadri and R.M. Westervelt, Phys. Rev. Lett. **66**, 2774 (1991); C-F. Chou, A.J. Jin, S.W. Hui, C.C. Huang and J.T. Ho, Science, **280**, 1424 (1998).

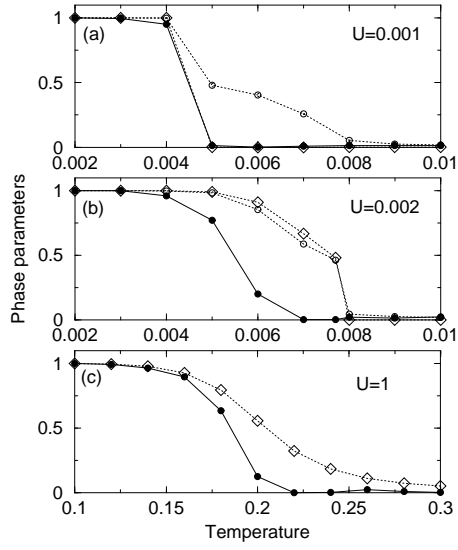


FIG. 1: Phase transitions at $f = 56^{-1}$ on a 112×112 lattice, for three values of pinning potential. Thick solid line (black dots) $= \rho_s/J$, thick dotted line (open circles) $= \phi_6$, thin dotted line (open diamonds) $=$ Bragg ratio in $S_0(\vec{k})$. Error bars are smaller than symbols. All energies are given in units of $2\pi J$.

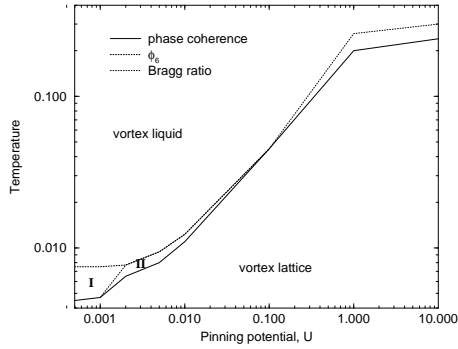


FIG. 2: Phase diagram for $f = 56^{-1}$ on a 112×112 lattice. Roman numerals I and II indicate the floating and the hexatic phases, respectively. All energies are given in units of $2\pi J$.

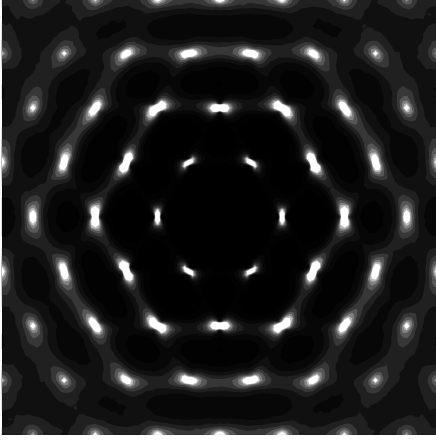


FIG. 3: Intrinsic structure function, $S_1(\vec{k})$, for the hexatic phase (II) at $k_B T/2\pi J = 0.007$ and $U/2\pi J = 0.002$.

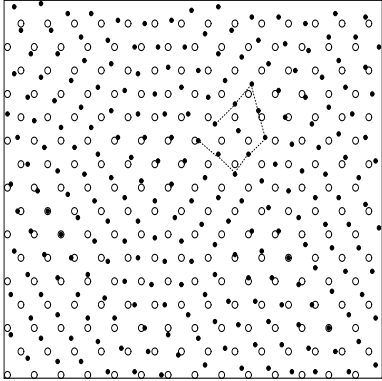


FIG. 4: Typical configuration (black dots) for the hexatic phase (II) at $f = 56^{-1}$ on a 112×112 lattice, at a temperature of $k_B T/2\pi J = 0.0067$ and pinning potential (open circles) $U/2\pi J = 0.0008$. Observe the presence of an unbound dislocation inside the Burgers circuit shown, and the absence of disclinations. Also notice the small number of pinned vortices (dot in circle).